Tellus (1992), *44B*, 358–370

Application of an atmospheric tracer model to high southern latitudes

By RACHEL LAW, IAN SIMMONDS and W. F. BUDD, *Department of Meteorology, University of Melbourne, Parkville, Victoria, 3052, Australia*

(Manuscript received 27 August 1991; in final form 11 February 1992)

ABSTRACT

We discuss the development of a global three-dimensional tracer model and use it to examine the atmospheric dispersal of passive tracer gases, particularly carbon dioxide, and their transport to Antarctica and the Southern Ocean. The tracer model is based on the University of Melbourne General Circulation Model and includes the effect of convective transport. Our results indicate the importance of a realistic treatment of the effect of convection. The model is applied to the dispersion of idealized distributions of tracer to determine atmospheric transport times. We examine particularly the time taken for the "tracer front" to reach the Antarctic coast and the South Pole in the case of clouds initialized at three latitudinal domains. The transport in all cases is seen to be very rapid south of about 45° S; this is due to the mixing associated with the strong and numerous transient disturbances at these latitudes in the Southern Hemisphere. The model is also used with an inverse technique and an annual mean carbon dioxide type distribution to deduce apparent sources and sinks of this gas. Net sources are found in the Northern Hemisphere and equatorial regions and net sinks in the Southern Hemisphere. This latter result is of considerable interest in view of the uncertainty of the CO_2 uptake by the Southern Hemisphere oceans.

1. Introduction

The study of the carbon budget of the atmosphere has been a relatively active scientific pursuit for many years. In the last few decades this budget has attracted increasing attention, associated with concerns that man's activities are disturbing the balance which has existed in recent centuries. There is no doubt that the atmospheric carbon dioxide loading is increasing (at present at the rate of about 1.5 ppmv per year) and that changes in this and other trace gases have significant impacts on the radiation balance of the earth (Hansen et al., 1985; Schlesinger, 1986). The potential severity of the many consequences of possible greenhouse warming dictates that it is a problem of considerable scientific importance.

Central to an understanding of the atmospheric carbon budget is the role of the atmosphere and ocean in transporting this constituent from source to sink regions. There is still considerable uncertainty in the contributions of, for example, deforestation and polar ocean uptake (Tans et al., 1989, 1990) and in addition the role of atmospheric transports is also rather poorly known in quantitative terms. The large-scale "turbulent" transfer of passive tracers in the atmosphere is a very complicated process and one that is ideally suited for study with numerical models. A number of numerical studies have been devoted to the atmospheric transport of trace gases. Some of the models used in these have been two-dimensional (solved in the height-latitude plane) (Tans et al., 1989; Enting and Mansbridge, 1991) and, as such, some of the conclusions derived from them may need to be treated with caution. Such models, by their nature, are not able to account for the potentially important longitudinal variations in both the source/sink distributions and the atmospheric circulation. Further, they are not able to adequately allow for the effect of transient disturbances, an omission which may be particularly severe in the mid and high latitudes of the Southern Hemisphere. Three-dimensional models, while being computationally more expensive, explicitly treat these features and have been used in a number of studies of trace gas and pollutant transport (e.g., Fung et al., 1983; Fung, 1986; Jacob et al., 1987; Prather et al., 1987; Pudykiewicz, 1989; Heimann and Keeling, 1989, and Tans et al., 1990). Many of these experiments have been performed with three-dimensional winds and information about convection provided by the General Circulation Model (GCM) developed by the Goddard Institute for Space Studies (GISS). We believe there is value in conducting studies with an independent model and GCM winds. Our model uses a somewhat different treatment of convection and of horizontal diffusion. In addition, the Melbourne University GCM, which provides the winds for our tracer model, appears capable of representing the vigorous circulation in the southern midlatitudes associated with the deep circumpolar Antarctic surface pressure trough and strong westerlies. This is of great importance for the rate of trace gas transport to Antarctica. It is also possible to use analysed winds from observations as has been done by Heimann and Keeling (1989).

The aim in the present paper is to provide a brief description of a tracer model derived from the University of Melbourne GCM and to report on some atmospheric tracer experiments we have performed with it. As described in the next section the code of the tracer model, and the winds with which it is forced, are derived from the GCM described by Simmonds (1985), which has been shown to produce creditable simulations of not only climate means (Simmonds et al., 1988; Simmonds, 1990) but also variability, including the simulation of individual cyclone behaviour (Simmonds et al., 1990; Murray and Simmonds, 1991), particularly at high southern latitudes. In this paper we are particularly interested in transport of tracer material to the Antarctic continent. One of the unique characteristics of the sub-Antarctic region is the presence of very intense baroclinic disturbances which have an almost-uninterrupted longitudinal domain. These transient waves effect massive poleward transports around the entire hemisphere, a total structure which has no counterpart in the Northern Hemisphere. We hypothesize that southward transport of a tracer is much more rapid when it reaches the midlatitudes of the Southern Hemisphere. In the sort of experiments we wish to perform, the importance of the quality of the model winds and variability cannot be overemphasized in regard to atmospheric transport of constituents to and from Antarctica.

In addition to carbon dioxide transport, the model is also of particular interest in regard to applications to Antarctic tropospheric chemistry such as the following. A large part of the atmospheric pollutants in the Antarctic are transported from the northern hemisphere by mechanisms that can be studied by the model. Antarctic atmospheric characteristics, such as low stratospheric ozone concentrations, can be transported northwards from the breakdown of the Antarctic vortex.

2. The tracer model

The model solves the tracer continuity equation in the form

$$\frac{\partial C}{\partial t} = -\nabla_\sigma \cdot \boldsymbol{u}C - \frac{\partial \dot{\sigma} C}{\partial \sigma} + {}_{\mathrm{h}}F_{\mathrm{C}} + {}_{\mathrm{v}}F_{\mathrm{C}}$$

$$+ \text{convection} + \text{source},$$

where C is the tracer mixing ratio, $-\nabla_\sigma \cdot \boldsymbol{u}C$ is the flux convergence on constant σ levels, $-\partial\dot{\sigma}C/\partial\sigma$ is the vertical flux convergence, ${}_{\mathrm{h}}F_{\mathrm{C}}$ is the horizontal diffusion of tracer and ${}_{\mathrm{v}}F_{\mathrm{C}}$ is the vertical diffusion of tracer. ${}_{\mathrm{h}}F_{\mathrm{C}}$ is given as $K\nabla^2 C$ with K set to $1.5 \times 10^5 \mathrm{~m}^2 s^{-1}$. The vertical diffusion is parameterized by the same mixing length method as used by McAvaney et al. (1978) which is appropriate for other quantities such as mass, heat, momentum and moisture.

The framework of the model is derived from the University of Melbourne General Circulation Model (GCM) (Simmonds, 1985; Simmonds et al., 1988). This is a spectral, rhomboidal (21 wave) model, with nine layers in the vertical, which can be used for both "perpetual" month and seasonal simulations. The full GCM can be used to calculate tracer transport but for a passive tracer it is more economical to also create a separate tracer model. This allows a large number of simulations to be run without having to recalculate the other meteorological parameters that a GCM produces. Instead, these parameters, such as wind and temperature fields, are taken as daily input to the tracer model and are linearly interpolated to each timestep as required. The impact of this interpolation on the tracer transport has been tested by comparison with the transport calculated by including the tracer in the full GCM. Initial results indicate that transport is somewhat slower if the interpolated fields are used and the reasons for this are still under investigation. The procedure for calculating tracer transport in the tracer model is similar to that used to transport moisture in the GCM with the exception of the method used to compute the vertical advection. In the GCM the finite differences are chosen to give greatest accuracy in the results whereas in the tracer model a conservative form of the vertical finite differences is used as this gives better tracer mass conservation. These schemes are described in Hoskins and Simmons (1975) and Williamson (1988).

2.1. *Convection*

One of the most difficult problems in atmospheric modelling is the determination of the appropriate treatment of the effects of sub-grid processes. Convection is one such process and it is known to play a very important role in the vertical redistribution of energy, particularly in the tropics. There is considerable debate as to how it should be "parameterized" in GCMs. It is clear that convection has an important impact on the distribution of passive tracers and hence the process should be included in tracer models. The difficulty in treating the effects of convection in these models is greater than in GCMs since the large-scale vertical thermal and moisture profiles are not, in general, known at all times as is the case in GCMs. Therefore, the approach we have taken is to use the monthly statistics of dry and moist convection generated by the control seasonal run of the parent GCM. This is similar to the methods used in the GISS tracer model (Fung et al., 1983; Prather et al., 1987) where the parameterizations are also based on convection statistics. However the methods used to transport the tracer vertically differ. The GCM uses a modified form of moist convective adjustment to parameterize convection following Manabe et al. (1965). This assumes two processes: dry convection when adjacent layers are unstable and unsaturated and moist convection when adjacent layers are unstable and saturated. In the case of dry convection, a temperature adjustment is made to give a dry adiabatic lapse-rate. This adjustment is done at each unstable pair of levels in turn. The statistics collected for dry convection is the proportion of the time that any given grid point in a layer participates in dry convection with the layer above. In the moist case an adjustment is made, to the moist adiabatic lapse-rate, over a block of unstable layers. Thus the moist convective cases are counted for 21 (viz. layers 1–2, 1–3, ..., 1–7, 2–3, ..., 6–7) different blocks of layers, with the maximum height of convection being layer 7.

The transport of tracer by convection in the tracer model is performed at every timestep. To implement this we assume that the proportion of the area of the grid box that takes part in convection every timestep is equivalent to the proportion of time the whole grid box takes part in convection during one day. The transport is performed by adjusting the tracer vertical profile, over the layers that are involved with convection, towards the mean for those layers. Hence the convectively adjusted tracer concentration at level k is given by

$$C_{\text{new}}(k) = C_{\text{old}}(k) + P(\theta, \lambda, k_{\text{b}}, k_{\text{t}}) \times (C_{\text{mean}} - C_{\text{old}}(k)),$$

where C_{mean} is the weighted mean (by layer mass) of the tracer mixing ratio and $P(\theta, \lambda, k_{\text{b}}, k_{\text{t}})$ is the

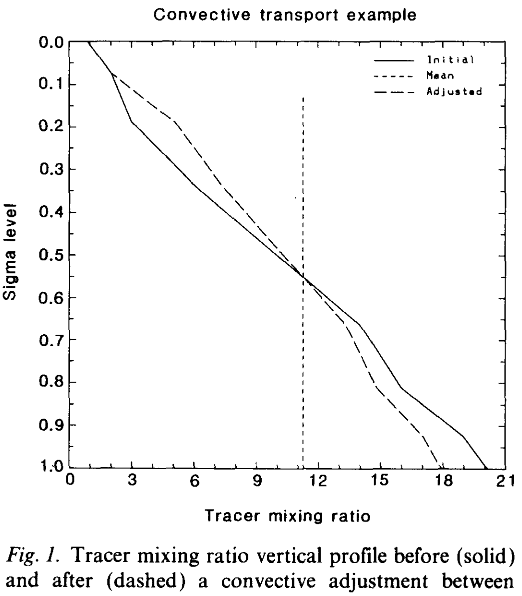

Fig. 1. Tracer mixing ratio vertical profile before (solid) and after (dashed) a convective adjustment between layers one ($\sigma = 0.991$) and seven ($\sigma = 0.188$) with $P = 0.25$.

proportion of time any given grid point (at latitude θ, longitude λ) and set of layers, defined by k_b, the bottom layer and k_t, the top layer, takes part in convection. This process is repeated for each of the 21 sets of layers at each timestep. In the "perpetual" month case (i.e., fixed solar declination, sea surface temperature etc.) the monthly mean statistics are used whereas in the seasonal model these monthly means are taken as applicable at the mid-point of the month and are linearly interpolated to daily values. A simple example is given in Fig. 1 for convection between layers one and seven and P assuming a value of 0.25 and $k_b = 1$, $k_t = 7$. This shows how adjusting the tracer profile towards the mean is equivalent to transporting the tracer vertically.

Figs. 2 and 3 show the seasonal variation (January and July) in the zonally-averaged convection statistics. The cross-sections display the percentage of timesteps that any given layer takes

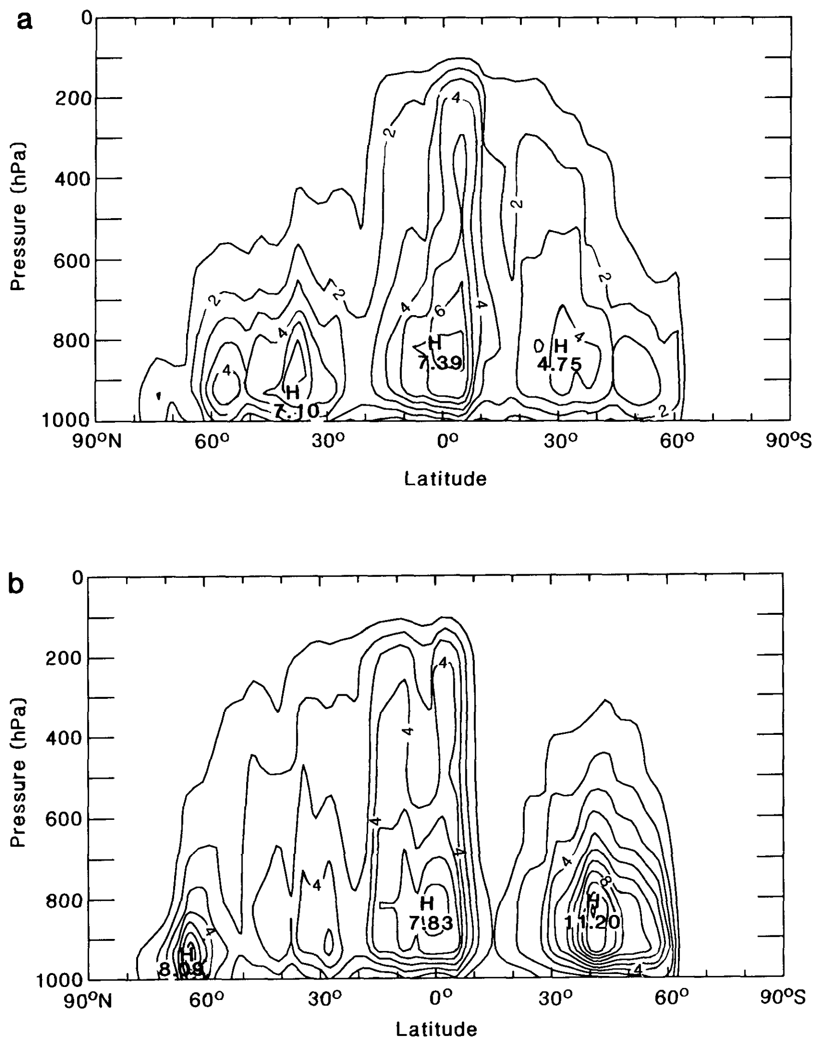

Fig. 2. Percentage of timesteps that each layer takes part in moist convection for (a) January and (b) July. Contour interval is 1%.

part in moist (Fig. 2) or dry (Fig. 3) convection calculated as

$$S(k) = \sum_{k_b} \sum_{k_t} P(\theta, \lambda, k_b, k_t),$$

where the summation indices range only over the values for which $k_b \leqslant k \leqslant k_t$. The plots show that moist convection occurs more frequently than dry convection at all but the lowest layers and is much deeper, reaching 200 hPa in tropical regions. Moist convection also shows a strong seasonal dependence with deeper convection over the summer hemisphere than the winter hemisphere. Convection is seen to be suppressed in the region of the descending branch of the dominant Hadley cell. The local maximum of convection around 40–60° in the winter hemisphere is probably associated with the destabilising influence of cold air moving off the polar ice or snow covered land

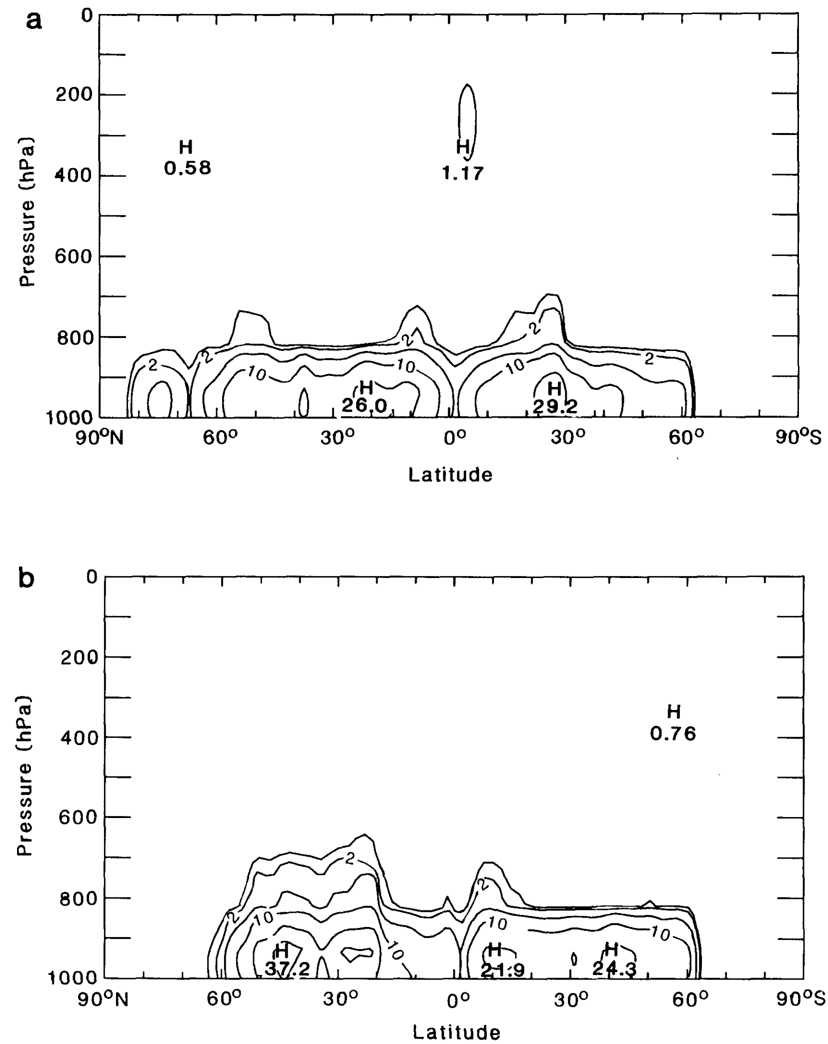

Fig. 3. Percentage of timesteps that each layer takes part in dry convection for (a) January and (b) July. Contours are 1, 2, 5, 10, 20, 30%.

and over relatively warm ocean in the region of mean vertical circulation between the Ferrel and Polar cells.

Figs. 4 and 5 give an indication of the geographical distribution of convection. The former shows the frequency of moist convection which extends through at least four layers while Fig. 5 shows the frequency of dry convection between layers one and two (where most dry convection occurs). The plots show a tendency for convection to occur in the tropics and over summer land surfaces.

The effect of convective transport can be seen in Fig. 6. This shows the difference in the zonally-averaged tracer distribution between two tracer runs, one with convection and one without. The tracer runs were for a one day period with July forcing and an initial distribution of constant tracer mixing ratio, of value 50 units, in the bottom four model levels ($\sigma = 0.664$ and below) and zero concentration above. The positive differences above negative ones indicate the extra vertical transport provided by convection. The vertical

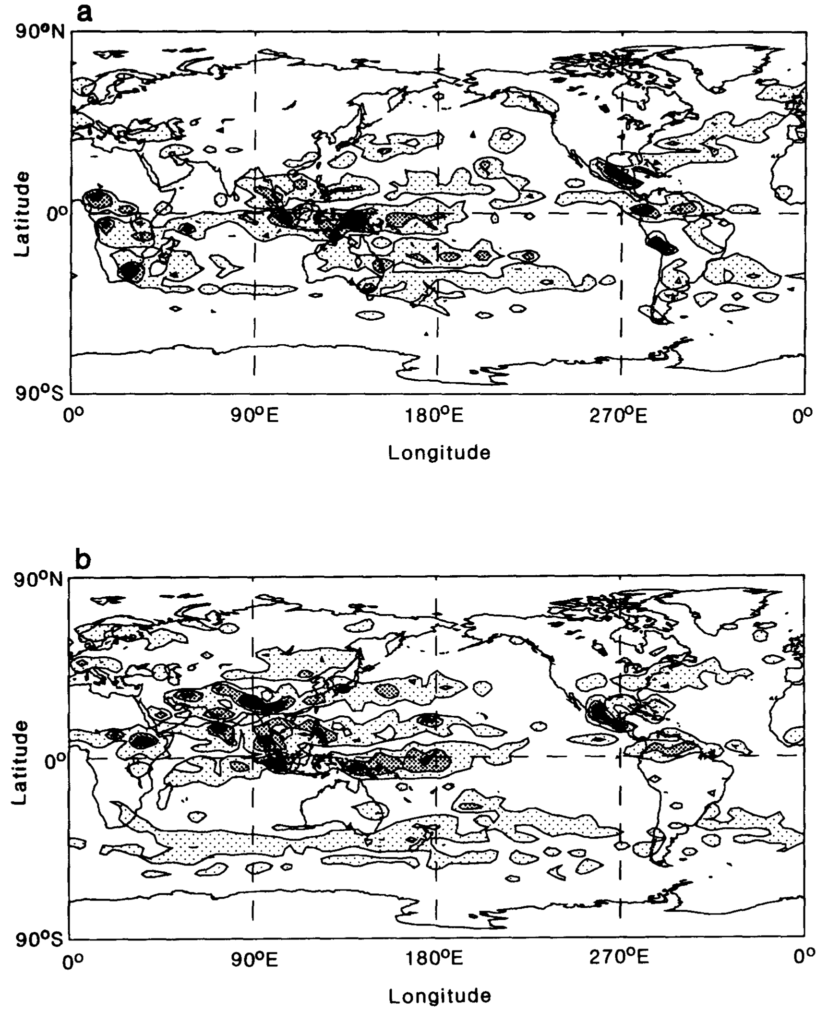

Fig. 4. Frequency of moist convection which extends through at least four layers for (a) January and (b) July. Light stippling is between 0.01 and 0.05, heavy stippling is between 0.05 and 0.1 and solid black is greater than 0.1.

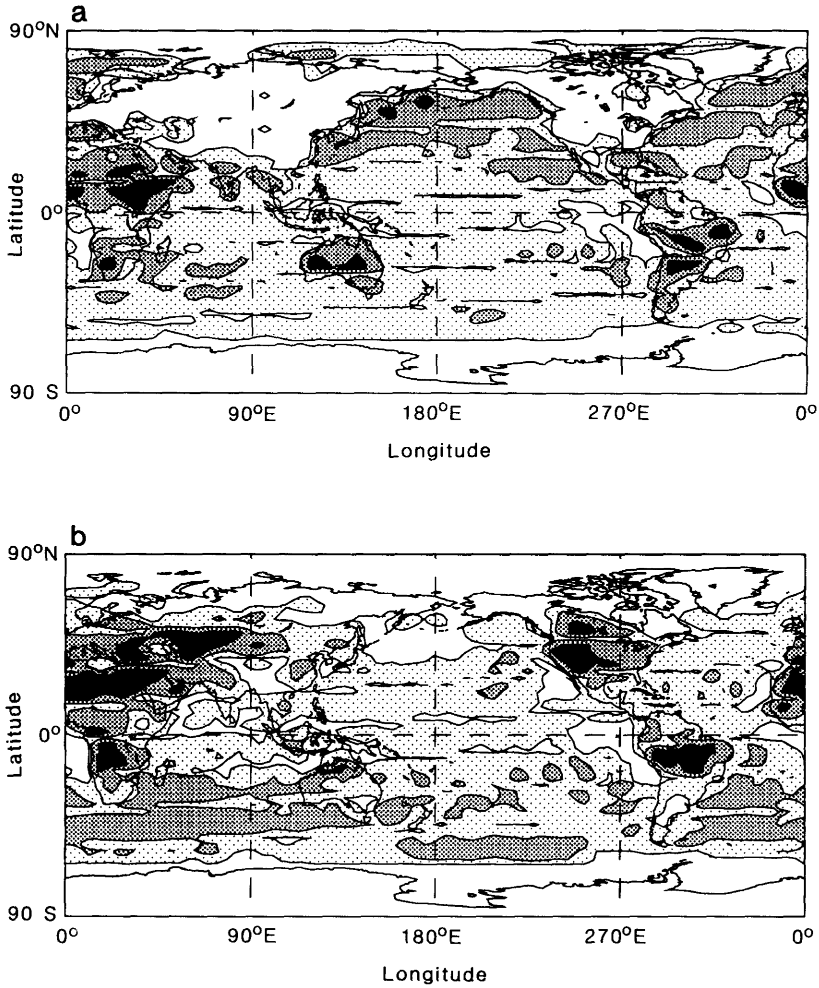

Fig. 5. Frequency of dry convection between layers one and two for (a) January and (b) July. Light stippling is between 0.01 and 0.2, heavy stippling is between 0.2 and 0.75 and solid black is greater than 0.75.

extent of the differences reflects the varying depth of convection at different latitudes. When comparisons are made with tracer transport in the full GCM, there is some indication (not shown) that the parameterization results in too much convective transport. Heimann and Keeling (1989) detected a similar bias in their use of the GISS model scheme and found it necessary to scale down the convective parameterization to fit with carbon dioxide observations.

Before proceeding we report on some preliminary analysis we performed for the purpose of validating the model. To effect this we have performed an experiment similar to that of Prather et al. (1987), who forced their model with a source proportional to the global electric power consumption and studied the transport of chlorofluorocarbons as related to observed distributions. The latitudinal profile of the zonally and vertically averaged tropospheric concentrations of an artificial tracer is not shown here but is almost identical to that obtained by Prather et al. when they included horizontal diffusive mixing in their model (their Fig. 2). The importance of this is that the

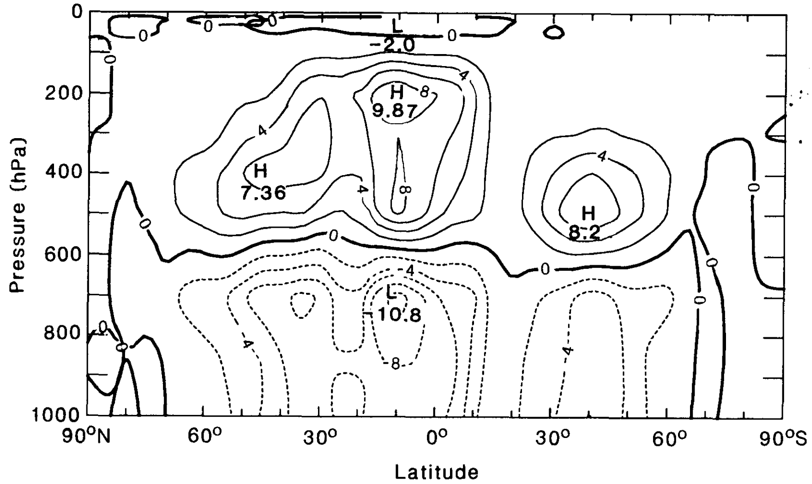

Fig. 6. Difference of zonally averaged tracer mixing ratio after one day in experiments with and without convection. Contour interval is 2 units. The initial distribution had a tracer mixing ratio of 50 units in the bottom four model layers.

model used by Prather et al. has been shown (by Jacob et al. (1987)) to be capable of accurately simulating the latitudinal distribution of ^{85}Kr. By implication the transport and mixing characteristics of our present model are validated (using a diffusion coefficient which is considerably smaller than that used by Prather et al.).

3. Simple experiments to test the behaviour of the model

The model has been run with a number of simple initial distributions and no sources or sinks. This has allowed the determination of transport times within the atmosphere and in particular the impact of distant sources on Antarctica, a region free from local pollution. Three initial distributions have been used, positioned in the northern and southern mid-latitudes and in the tropics, with zero values elsewhere in each case. The distributions were constant in the vertical, zonally symmetric and covered the latitude bands 44–54° N, 5° S–5° N and 44–54° S. Each of these experiments, denoted by N, T and S respectively, was run using January winds and convection and July winds and convection. Each case shows an initial rapid decrease in the tracer maximum and a gradual dispersal throughout the atmosphere. Since the experiments are run with no sources and sinks the tracer tends towards a globally uniform distribution. An approximately uniform distribution is seen after 150 days in the tropical case compared with about 300 days in the northern mid-latitude case.

The southward progression of the tracer "front" in July is presented in Fig. 7. This displays the time taken for each latitude south of the initial distribution to reach a zonally-averaged tracer concentration of 67% of the (conserved) globally averaged value in the experiment. (Note that the tracer will everywhere asymptotically approach this average value. We have chosen this normalized definition of the "front", rather than express it in terms of tracer concentration, as the asymptotic value in N and S differs from that in T.) The results are presented for 850 and 200 hPa and indicate the southward extent of significant amounts of tracer at any given time at these heights. In case N, initially the tracer at the lower level moves southward fastest but just north of the equator the upper level overtakes. This reflects the influence of the upper branch of the Hadley cell. Case T shows a similar pattern with the upper levels leading the lower levels between 10 and 40° S. A remarkable feature of the Figure is the dramatic increase in transmission speed when the tracer front reaches the southern midlatitudes, this feature being particularly marked at the lower levels. This speedup

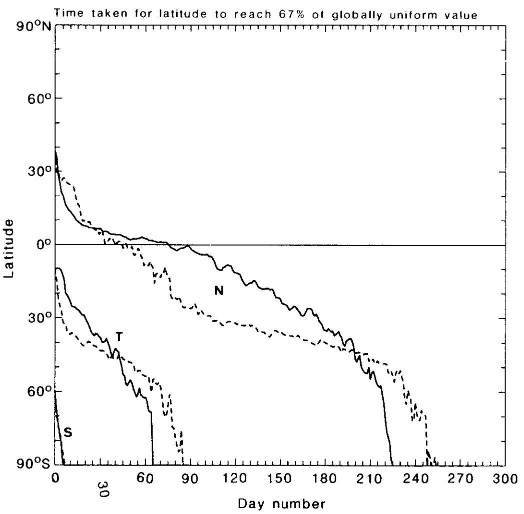

Fig. 7. Southward extent of tracer mass, defined by the time taken for each latitude to reach 67% of the asymptotic globally uniform concentration in experiments N, T and S (in which the initial tracer clouds were located in the northern midlatitudes, tropics and southern midlatitudes, respectively). Daily values are shown for 850 hPa (solid) and 200 hPa (dashed). The experiments were forced with July winds.

Table 1. *Transport times (in days) from the northern midlatitudes, tropics and southern midlatitudes (experiments N, T and S, respectively)*

		70° S				90° S			
		January		July		January		July	
	hPa	850	200	850	200	850	200	850	200
N	10%	85	91	81	89	90	102	87	96
	67%	227	281	220	238	227	294	225	248
T	10%	31	33	25	31	35	41	29	32
	67%	85	126	65	73	90	134	65	85
S	10%	1	1	2	1	5	6	5	6
	67%	2	1	2	2	5	15	6	7

Presented is the time to reach 70 and 90° S at 850 and 200 hPa for January and July conditions. The times are given for the "10%" and "67%" fronts and are times after which the zonally-averaged tracer concentration first exceeds 10% and 67% of their asymptotic values.

is associated with the strength of the southern midlatitude transient eddies and indicates the importance of using winds in this region which reflect the vigorous nature of the actual circulation there. The overall transport time to the South Pole is approximately eight months for case N, ten weeks for case T and one week for case S.

Some of the information on transport times to the Antarctic coast (70° S) and the South Pole in the three experiments for both January and July simulations is summarized in Table 1. The Table presents these times for the 200 and 850 hPa levels and for two "fronts" defined as 10% and 67% of the asymptotic value. In all but two cases, the fronts at 850 hPa reach these southern latitudes before their counterparts at 200 hPa. The "67% front" takes typically three times longer than the "10% front" to reach the Antarctic. Notice also that, for the most part, transport times are longer in the southern summer.

4. Experiments using a carbon dioxide type distribution

To increase our understanding of the atmospheric transport of carbon dioxide, some experiments have been performed based on a north-south tracer distribution similar to the mean annual observed distribution of this gas. This is illustrated in Fig. 8 by curve A and is taken from Enting and Mansbridge (1991). For simplicity the distribution has been taken as constant in the vertical and zonally symmetric.

Meridional tracer transport can be divided into three components by breaking v, the meridional velocity, and C into mean and varying components in both time and space. For v this gives

$$v = \bar{v} + v', \qquad \bar{v} = [\bar{v}] + \overline{v^*},$$

where $\bar{v}$ is the time mean, v' is the deviation from the mean, $[v]$ is the zonal mean and v^* is the deviation from the zonal mean. This gives for the mean meridional tracer transport at any given level:

$$[\overline{vC}] = [\bar{v}][\bar{C}] + [\overline{v^*C^*}] + [\overline{v'C'}],$$

where $[\bar{v}][\bar{C}]$ is the transport due to the mean meridional circulation, $[\overline{v^*C^*}]$ the transport due to stationary eddies and $[\overline{v'C'}]$ that due to transient eddies. Two experiments were run from the initial distribution described above, without any sources or sinks, to determine the influence of the transient eddies. Both were run for 100 days, the first using daily July winds, the second using the July mean monthly wind. This second run, therefore, eliminates the effect of transient eddies since $v' = 0$. The results (Fig. 8) show for the first case an increasing gradient between 10°N and 10°S, decreasing mixing ratios in the Northern Hemisphere and increasing mixing ratios in the Southern Hemisphere. This gives an overall reduction in the difference in tracer mass between hemispheres. In particular around 60°N the mixing ratio decreases almost 0.9 ppm over 100 days. The second plot in Fig. 8 shows the results using the monthly mean wind. The mixing ratios between 30°N and 30°S are very similar to previously but in the mid and high latitudes deviations from the initial distribution are much smaller than in the case using the daily winds. At 60°N the mixing ratio has only dropped 0.3 ppm in 100 days. This indicates that the transport within the tropics is predominantly effected by the mean meridional circulation as expected with the strong Hadley cells. However at mid and high latitudes the transport must be dominated by the transient eddies as shown in the different results in this region. The importance of including the effects of the transients in tracer studies can be appreciated from these results.

Assuming that the time variation of a tracer distribution is known, it should be possible to deduce the sources required to maintain that distribution. For example, the observed time series of carbon dioxide concentrations could be used as the known distribution. However for simplicity the method has first been tested by assuming the tracer distribution remains constant in time equal to the distribution shown by curve A in Fig. 8. The sources have been deduced by running the July tracer model as previously but each timestep (15 minutes) resetting the tracer distribution at the bottom layer (only) to the original distribution. A similar procedure has been employed by Tans et al. (1989). The total source is the sum of these adjustments made every timestep. The calculated sources have been averaged over seven consecutive 31-day periods. The zonal average, converted to a flux of carbon into the bottom of the atmosphere per year is plotted in Fig. 9. Note that the flux area unit is 2.55×10^{13} m^2, the magnitude of the 20 globe-covering equal area boxes used by Tans et al. (1989). The results show that it takes approximately 90 days to reach the source equilibrium distribution. This adjustment time is due to the upper levels being allowed to develop

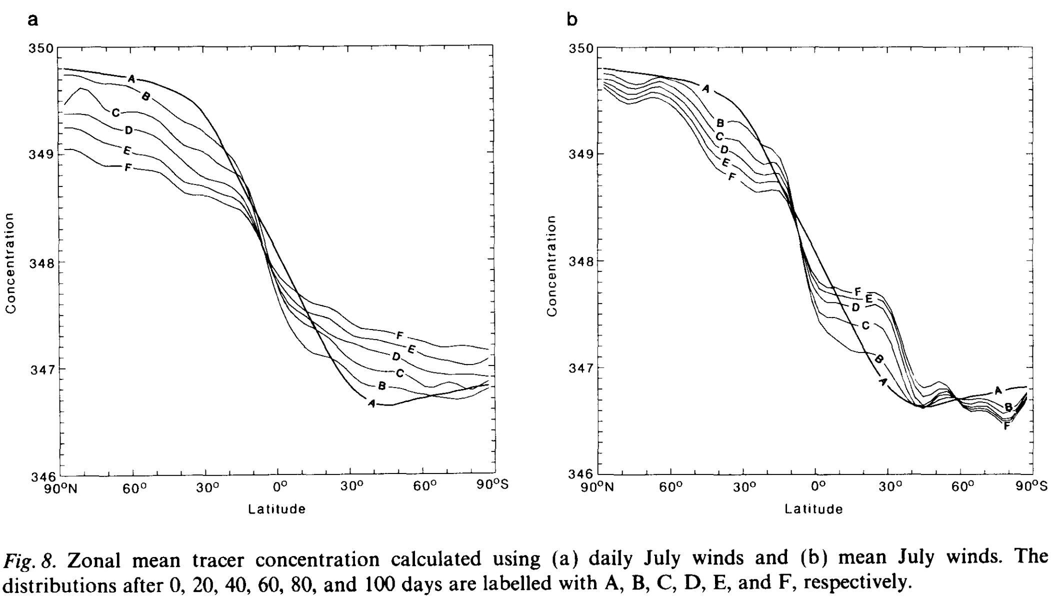

Fig. 8. Zonal mean tracer concentration calculated using (a) daily July winds and (b) mean July winds. The distributions after 0, 20, 40, 60, 80, and 100 days are labelled with A, B, C, D, E, and F, respectively.

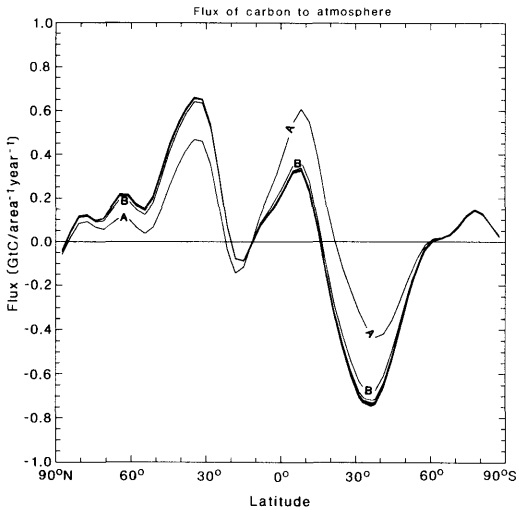

Fig. 9. Zonal mean carbon flux averaged over seven consecutive 31-day periods and calculated using July winds. The units are GtC $(2.55 \times 10^{13}\ m^2)^{-1}$ year^{-1}. The time-scale of the convergence is such that only the curves for the first two periods (curves A and B) are clearly differentiable and these are the only two labelled.

freely from an initialized state equal to the surface layer. The plot shows sources in the Northern Hemisphere with a smaller peak at the equator and a strong sink in the Southern Hemisphere. This is as expected, with the sources having to balance the tendency to a weakening gradient due to mixing by the circulation. This finding is of considerable interest in light of the present uncertainty in quantifying the amount of CO_2 uptake by the southern oceans (e.g., Tans et al., 1989, 1990). The net source and sink are both about 4.0 GtC year^{-1}. The results give some support to the concept of a substantial sink for CO_2 in the Southern Hemisphere oceans. The response of the upper levels is seen in the vertical cross-section of zonal mean tracer concentration for day 187 (Fig. 10). The plot shows decreasing concentrations with height in the Northern Hemisphere and the reverse in the Southern Hemisphere. This is consistent, both in sign and magnitude, with observations from aircraft (Beardsmore et al., 1984; Gammon et al., 1985).

Sources have also been calculated using the January circulation to force the model. The sources deduced for the last 31 days of this run have been combined with the equivalent July results to provide an estimate of the annual mean source. The global apparent source distribution for this forced zonally uniform distribution is shown in Fig. 11, again in terms of the flux of carbon. This shows local areas of maximum source over North America and in the North Indian region. Maximum sinks occur around Peru in South America and over southern Africa. These meridional variations are a result of the particular structure of

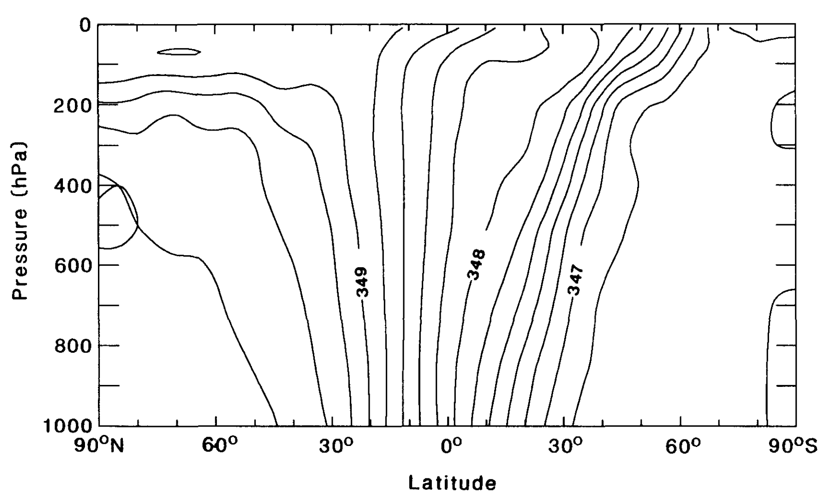

Fig. 10. Zonal mean tracer concentration for day 187 of the experiment with the lowest level tracer constrained and using July winds. Contour interval is 0.2 ppm.

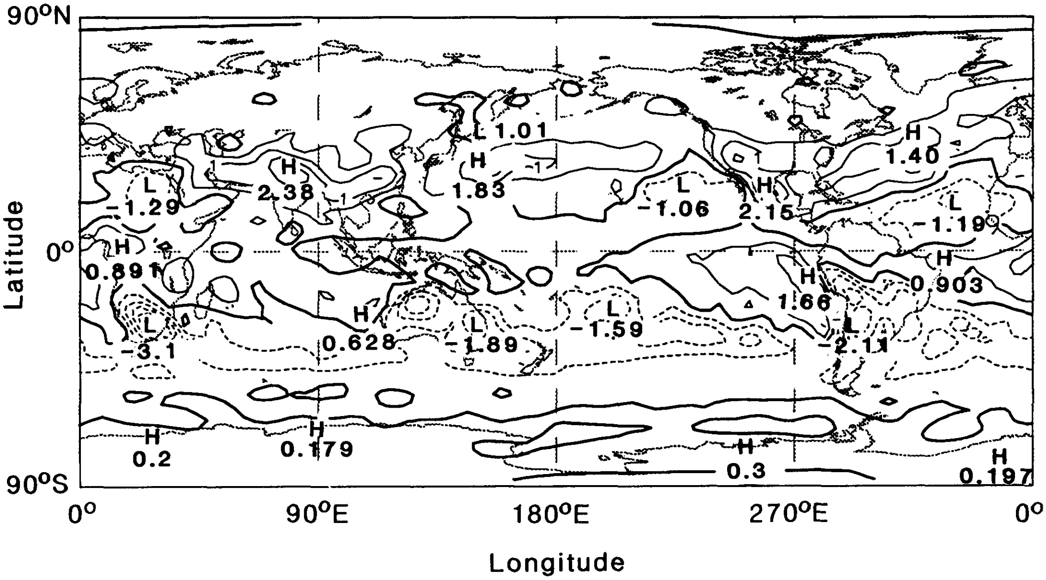

Fig. 11. Average deduced source for day 187–217 January and July. Contour interval is 0.5 GtC (2.55×10^{13} m^2)$^{-1}$ year^{-1}.

the circulation. For example, the maximum over North India is thought to be required to offset the northward transport of air with lower tracer mixing ratio during the monsoon season. A central point to be made here is that considerable asymmetry would be required in the sources/sinks of the tracer in order to maintain a zonally uniform concentration at the surface.

5. Conclusions

The results presented show the potential of three-dimensional tracer models to increase our understanding of the transport of atmospheric constituents. Some of the difficulties of tracer modelling, in particular the treatment of convection, have also been discussed. The tracer model currently being used at the University of Melbourne has produced realistic tracer distributions in experiments with simple initial distributions. These results have been used to calculate typical north-south transport times with particular reference to the growth of tracer concentration in Antarctica. A finding of particular importance here is the rapid speedup of the "tracer front" when it enters the baroclinically active regions of the southern midlatitudes. Once a tracer cloud has reached these latitudes travel times to the Antarctic continent are quite short. The influence of convection on tracer transport has also been addressed and is found to be large. Further work is being undertaken to test the sensitivity of the model results to the parameterization of this important subgrid process.

An annual mean carbon dioxide-type tracer distribution, specified as a function of latitude, has been used to show the importance of transient eddies for meridional transport in the midlatitudes. Also, initial results have been presented showing the implied sources when the initial distribution is kept fixed and not permitted to vary with longitude. They show a Northern Hemisphere and equatorial source and Southern Hemisphere sink. Another finding of considerable importance to come from this work is that significant asymmetry would be required in the sources/sinks of the tracer in order to maintain a zonally uniform concentration at the surface. Even though the CO_2 concentration would be expected to exhibit longitudinal variations there are too few data to prescribe the surface distribution across longitudes. Our results indicate that longitudinal spatial variations must be expected and there is a need for a more comprehensive observed data set to deduce the net surface fluxes. This work is ongoing. We are looking in particular at validating the deduced sources by running the tracer model freely from the initial distribution using the calculated source distribution. Future experiments will include the annual cycle and the growth rate of carbon dioxide in the atmosphere.

REFERENCES

Beardsmore, D. J., Pearman, G. I. and O'Brien, R. C. 1984. The CSIRO (Australia) *Atmospheric carbon dioxide monitoring program: surface data*. CSIRO, Div. of Atmospheric Res. Tech. Paper No. 6.

Enting, I. G. and Mansbridge, J. V. 1991. Latitudinal distribution of sources and sinks of CO_2: Results of an inversion study. *Tellus 43B*, 156–170.

Fung, I., Prentice, K., Matthews, E., Lerner, J. and Russell, G. 1983. Three-dimensional tracer model study of atmospheric CO_2: response to seasonal exchanges with the terrestrial biosphere. *J. Geophys. Res. 88*, 1281–1294.

Fung, I. Y. 1986. Analysis of the seasonal and geographical patterns of atmospheric CO_2 distributions with a three-dimensional tracer model. In: *The changing carbon cycle: a global analysis* (ed. J. Trabalka and D. Reichle). Springer-Verlag, 459–473.

Gammon, R. H., Sundquist, E. T. and Fraser, P. J. 1985. 3. History of carbon dioxide in the atmosphere. In: *Atmospheric carbon dioxide and the global carbon cycle* (ed. J. Trabalka). US Dept. of Energy. DOE/ER-0239, 25–62.

Hansen, J., Russell, G., Lacis, A., Fung, I., Rind, D. and Stone, P. 1985. Climate response times: dependence on climate sensitivity and ocean mixing. *Science 229*, 857–859.

Heimann, M. and Keeling, C. D. 1989. *A three-dimensional model of atmospheric CO_2 transport based on observed winds: (2) Model description and simulated tracer experiments.* Max-Planck-Institut für Meteorologie, Report No. 33. Hamburg, Germany.

Hoskins, B. J. and Simmons, A. J. 1975. A multi-layer spectral model and the semi-implicit method. *Quart. J. Roy. Meteor. Soc. 101*, 637–655.

Jacob, D. J., Prather, M. J., Wofsy, S. C. and McElroy, M. B. 1987. Atmospheric Distribution of ^{85}Kr Simulated With a General Circulation Model. *J. Geophys. Res. 92*, 6614–6626.

Manabe, S., Smagorinsky, J. and Strickler, R. F. 1965. Simulated climatology of a general circulation model with a hydrologic cycle. *Mon. Wea. Rev. 93*, 769–798.

McAvaney, B. J., Bourke, W. and Puri, K. 1978. A global spectral model for simulation of the general circulation. *J. Atmos. Sci. 35*, 1557–1583.

Murray, R. J. and Simmonds, I. 1991. A numerical scheme for tracking cyclone centres from digital data. Part II: Application to January and July GCM simulations. *Aust. Met. Mag. 39*, 167–180.

Prather, M., McElroy, M., Wofsy, S., Russell, G. and Rind, D. 1987. Chemistry of the Global Troposphere: Fluorocarbons as Tracers of Air Motion. *J. Geophys. Res. 92*, 6579–6613.

Pudykiewicz, J. 1989. Simulation of the Chernobyl dispersion with a 3-D hemispheric tracer model. *Tellus 41B*, 391–412.

Schlesinger, M. E. 1986. Equilibrium and transient climatic warming induced by increased atmospheric CO_2. *Climate Dynamics 1*, 35–51.

Simmonds, I. 1985. Analysis of the "spinup" of a general circulation model. *J. Geophys. Res. 90*, 5637–5660.

Simmonds, I., Trigg, G. and Law, R. 1988. The Climatology of the Melbourne University General Circulation Model. Pub. No. 31, Department of Meteorology, University of Melbourne, 67 pp. [NTIS PB 88 227491.]

Simmonds, I. 1990. Improvements in General Circulation Model performance in simulating Antarctic climate. *Antarctic Science 2*, 287–300. (Note Correction in vol. 3, p. 230.)

Simmonds, I., Indusekharan, P. and Murray, R. J. 1990. A comparison of modelled and observed daily variability in the southern extratropics. *Aust. Met. Mag. 38*, 261–270.

Tans, P. P., Conway, T. J. and Nakazawa, T. 1989. Latitudinal Distribution of the Sources and Sinks of Atmospheric Carbon Dioxide Derived From Surface Observations and an Atmospheric Transport Model. *J. Geophys. Res. 94*, 5151–5172.

Tans, P. P., Fung, I. Y. and Takahashi, T. 1990. Observational constraints on the global atmospheric CO_2 budget. *Science 247*, 1431–1438.

Williamson, D. L. 1988. The effect of vertical finite difference approximations on simulations with the NCAR community climate model. *J. Climate 1*, 40–58.